01,03,05,10

Degradation of colossal magnetoresistance of europium hexaboride in the point contacts

© Yu.V. Goyunov

FRC „Kazan Scientific Center of RAS“,
Kazan, Russia

E-mail: gorjunov@kfti.knc.ru

Received December 28, 2025
Revised December 28, 2025
Accepted January 16, 2026

Point contacts fabricated of EuB_6 semi-metal known for its colossal magnetoresistance at low temperatures were prepared. EuB_6 is also featuring a very high melting temperature of ($\sim 2500\,^{\circ}C$) and high hardness (~ 40 GPa/M) which depends on the crystallographic index. The geometry of the obtained point contacts is estimated and the temperature dependences of their magnetoresistance are measured, while monitoring the behavior of the magnetoresistance of a bulk sample. It is found that the temperature dependences of the magnetoresistance for bulk materials and point contacts are similar in terms of characteristic temperatures indicating the formation and ordering of spin polarons, and also have a similar temperature dependence of magnetization obtained after measurements of electron spin resonance. Yet, for the point contacts, the effective magneto-resistance values are significantly lower than their values for the same bulky material. The point contacts, in addition to the singularity near 15.5 K associated with the ferromagnetic ordering of magnetic polarons, also have a singularity near the temperature of 23 K. These findings are interpreted as a consequence of pinning of spin polarons inside the contacts at temperatures of 15.5 K and 23 K, which inhibits the shift of the magnetic interface boundaries when the contact size approaches the correlation length of the nematic magnetic phases in EuB_6.

Keywords: magnetic phase separation, colossal magnetoresistance, exchange interaction, spin polarons, quantum nematic.

DOI: 10.61011/PSS.2026.02.63375.355-25

1. Introduction

In 90s a phenomenon of colossal magnetoresistance was discovered in compounds of transition metals (Mn, Cu, Fe) [1–4] or rare-earth metals (La, Eu) [5,6] featuring a mixed ion-covalent bond where the collectivization of electrons of the cation and anion complexes occurs. Europium hexaboride, outlined in this report and which is a classic material on which a huge number of studies of the colossal magnetoresistance phenomenon have been performed, has a simple cubic lattice and a magnetic ion Eu^{2+} in a purely spin $^8S_{7/2}$ state, with its s-electrons almost completely transiting into the valence band towards boron ions, nevertheless, leaving a small number of free electrons in the conduction band. However, it is this small number of electrons that is the main player in scenarios and models explaining the nature of the phenomenon of colossal magnetoresistance.

In the last twenty years, the concepts of small-scale magnetic or charge phase separation [3–7] and the formation of magnetic polarons [6,8–11] have underpinned the ideas about the nature of this phenomenon. In recent years these systems have been highlighted as the spin nematic materials in some region of T-H diagram [12–16]. According to the approach developed in studies by K.I. Kugel et al. [17] based on Falicov and Kimball model [18], the electronic structure of a material consisting of two conduction bands with various kinds of carriers that due to the exchange interactions produce the regions with a single type carrier.

In case of EuB_6, as well as other mentioned compounds, on the one hand, the closest relationship between the valence and magnetic states of the cation causes a variety of magnetic properties of the compound. On the other hand, the network of valence bonds ensuring the stability of the compound lattice and determining its symmetry, and existing as a kind of spatial structure of allowed orbitals on which valence electrons can be located, is on the verge of depletion, beyond which another type of crystal lattice is realized. At the same time, due to the formation of vacancies (i.e., the breaking of bonds in the network of valence orbitals) in both europium and boron, the cubic structure is realized in a wide area near the stoichiometric composition. Low electron density, ambiguity of the crystal structure and superposition of the valence band on the conduction band underlie a huge variety of magnetic and electronic properties, while the slightest changes in the number of valence electrons lead to local distortions of the compound's crystal structure. As mentioned in [3,4], the study of electronic transport properties of systems with small-scale phase separation builds bridges between the physics of strongly correlated electronic systems and mesoscopic physics, without which it is impossible to understand the phenomena occurring in nanostructures, on surfaces and other low-dimensional systems, in particular,

quantum dots and microcontacts (nanobridges). The latter issues turn out to be insufficiently studied, except for the study of charge density distribution by tunneling probe microscopy [19]. Of course, this area is closely related to the application of microcontact spectroscopy method [20] in the study of the role of surfaces and defects in the small-scale magnetic phase separation of a quantum nematic, manifestation of surface energy at the interfaces of magnetic phases, modification of the spectra of phonons and magnons in small-scale phase separation due to quantum dimensional effects. However, this paper describes only technical issues of preparing the microcontacts EuB_6, their modification, and the difference between their properties and a bulk material that determine the correctness of the experiment.

2. Experiment

2.1. Preparation of samples

The microcontact samples were prepared by pressing a tip formed by three cleavages on the same planes against the cleavage along the planes (100). It is known that europium hexaboride, having a cubic lattice, cleaves along cleavage planes {100} and has a hardness close to that of corundum [21]. Therefore, there is reason to believe that a crystalline indenter having a tip in the direction of axis [111], being pressed by a soft spring holder to the plane (100), forms a Sharvin microcontact with it [22]. This geometry differs slightly from the geometry measured by Rockwell hardness method, which uses as an indenter a cone with a generatrix located at an angle 60° close to the angle of deflection of the edges ($\sim 55°$) converging at the top of a triangular pyramid formed by the angle of a cube. Thus, the idea with the experiment with such a contact turned into the following diagram as shown in Figure 1. The central crystal, faceted with cleavages {100}, with potential measuring contacts located on the long side of the plane (100), is glued onto the holder rod. Current contacts to this crystal are connected to its end planes from opposite sides by means of two crystal points, the axis [111] of which is close to the axis [010]. These crystals ~ 0.3 mm in size are glued to the ends of two brass spring holders using a drop of silver paste. These spring holders are located along the rod. The brass holders are 2×10 mm in size, with a thickness of 0.1 mm. The bulk crystal is 2.4×2.0 mm in size, with a thickness of 0.8 mm. Potential measuring contacts are also glued to the central crystal using silver paste. The potential contacts are made of aluminum conductors with a diameter of 0.05 mm. The distance between these potential contacts is ~ 1.5 mm. Silver paste resistance is $0.1-0.2\,\Omega$. Thus, the resistance of elements supplying current to the microcontacts is many times less than the resistance of the microcontacts themselves. A plate with intermediate contact pads was also located on the rod, from which insulated copper wires about 0.5 mm long and 0.1 mm in diameter were laid from the sample holder to the output of the continuous-flow cryostat.

2.2. Measurements of magnetoresistance

As can be seen from Figure 1, the measuring circuit consisted of a low-resistance part for measuring the potential on a bulk sample and a high-resistance part for measuring the potential on microcontacts. A standard four-contact circuit was used to measure the magnetoresistance in the low-resistance part of the structure. The same measuring current from the power supply ATH-1533 (Actacom), controlled by DC voltage and ballast resistance of $R_b = 1.3\,\text{k}\Omega$ was flowing through the two high-resistance microcontacts and the bulk sample (low-resistance part). Nanovoltmeter B2-38 (internal resistance of $3\cdot 10^7\,\Omega$, $I < 10^{-4}\,\mu$A) was used to measure the difference of potentials on the bulk sample (low-resistance part). Multimeter AM-1109 (Actacom, internal resistance of $1.2\cdot 10^7\,\Omega$) was used to measure the difference of potentials on some of the microcontacts (high-resistance part). The supply conductors are made of copper wire with a diameter of 0.1 mm. The measurements were carried out with the magnet power off and in a field of 0.78 T for two directions of the measuring current. The magnetic field had a direction from one microcontact to another, i.e. along [010] axis of the bulk sample. Helium continuous-flow cryostat was used to measured the temperatures within $10-300$ K. The temperature was measured by the thermocouple.

3. Experimental results

To find the optimal measuring current, the volt-ampere characteristics on the high-resistance and low-resistance parts of the sample were measured. The characteristics were linear themselves with a slight kink at zero current. A short-term measurement of the resistance of one microcontact at high current was made, corresponding to the voltage of 0.6 V (voltage at the multimeter during direct resistance measurement) at the current contact. This measurement showed that during around 10 seconds the initial resistance of $\sim 1\,\text{k}\Omega$ grew significantly. This was an evidence of a strong heating of the microcontact. After stopping the current supply to the microcontact and waiting for $2-3$ minutes in order to normalize the temperature of the microcontacts, repeated measurement of the resistance of the microcontact showed that after cooling, its resistance declined by about two times. This indicates that when a large current (about 2 mA) was flowing, the microcontact was settled and possibly fused. After crystallization a boundary of transition from orientation [100] to orientation [111] should have been set. After all measurements done, the locations of the indenter-contacts were thoroughly examined using a microscope. The examination showed that axis [111] of one of the indenters is close to the direction of axis [100] of the bulk material, and axis [111] of the second indenter forms with the axis [100] of the bulk material the angle around $15°-20°$. Obviously, when a point contact is heated by a high-density current, the heat generated in it is diverted to a solid angle $\pi/2$ into the indenter and

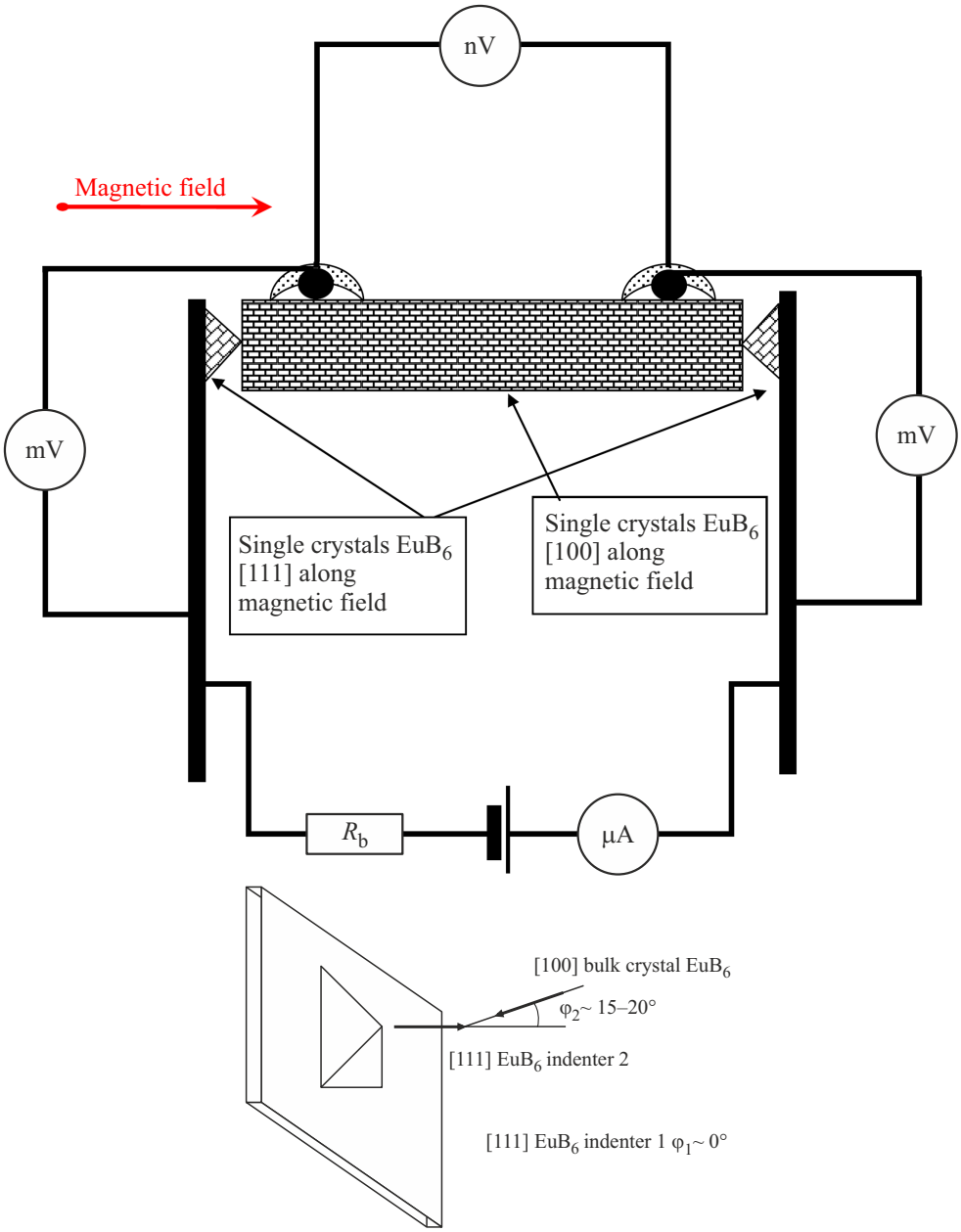

Figure 1. Diagram illustrating simultaneous measurement of the magnetoresistance of a bulk sample and microcontacts. The type of indenter-contacts is shown in the inset at the bottom.

to a solid angle 2π into the bulk material. Thus, the area of contact heating (respectively, melting in the case of temperatures above the melting point) will spread towards the indenter at a distance of $[(2\pi)/(\pi/2)]^{1/2} = 2$ times the spread in the bulk material. This means that when the melt solidifies, the contact recrystallizes as a continuation of the crystalline structure of the bulk material. On the indenter side, the microcontact should have an area rich in crystal structure defects caused by misalignment of crystallographic directions. This also means that the scattering of current carriers inside the microcontact will vary depending on the direction of electron movement through the contact. When moving away from a massive material along the direction [100] (and also along the direction of external magnetic field), the carrier flow will be partially ordered along this axis and have some ballistic component. When moving from the indenter side in the direction of [111] before entering the contact, the current carriers will experience numerous scattering in the defects when transiting towards [100] and the ballistic component will most likely be absent. It should be noted that in the microcontact, the regions in which the magnetic field is directed along [100] axis and along [111] axis (corresponding to the direction with maximum magnetic susceptibility and paramagnetic temperature) produce a serial electrical connection.

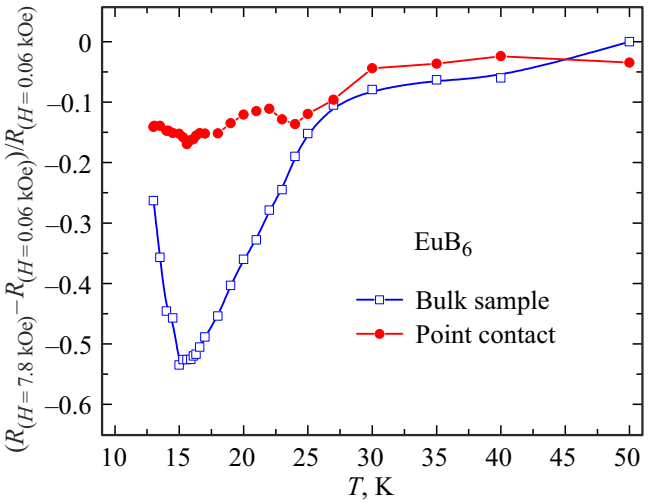

Figure 2. Temperature dependences of the relative magnetoresistance of the bulk sample and the first microcontact to this sample with the contact single-crystal oriented as shown in the inset in Figure 1. For $\varphi \sim 0°$.

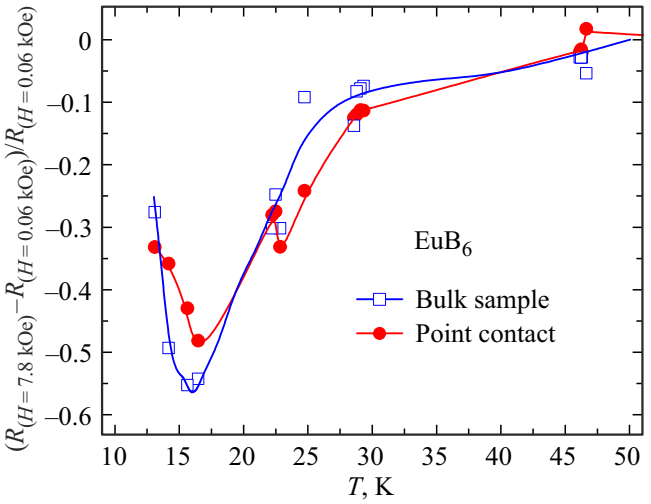

Figure 3. Temperature dependences of the relative magnetoresistance of the bulk sample and the second („damaged, overheated") microcontact to this sample with the contact single-crystal oriented as shown in the inset in Figure 1. For $\varphi \sim 15-20°$.

Figure 2 shows the simultaneously measured temperature dependences of the magnetoresistance of the bulk sample and the first microcontact. For the bulk sample, this dependence has a previously known form and in its shape is equivalent to the temperature dependence of the magnetization of a pure EuB_6 crystal obtained from ESR measurements [23–25]. For the microcontact this dependence is very weak, practically 5 times weaker, but it has two distinct singularities at the temperatures of ~ 23 K and ~ 15.5 K that was also observed in ESR measurements. The observed weakening of the temperature dependence of the microcontact magnetoresistance may be explained by taking into account the resistance of the supply Al and Cu conductors in the measuring circuit. However, this resistance is significantly less than the resistance of the contact itself. In addition, this weakening of the temperature dependence of the magnetoresistance is insignificant on the other microcontact.

Figure 3 shows the magnetoresistance dependence of the same bulk sample with the same contacts in the same circuit and the magnetoresistance dependence of the second („damaged") microcontact. The latter dependence turns out to be close to that of the bulk crystal, although somewhat weakened, and has features at the same temperatures of 15.5 K and 23 K. The initially observed weak dependence of the sample's potentials towards external magnetic field (from $+10°$ to $-60°$) is assumed to be erroneous, because it repeats small temperature fluctuations that occurred during its measurement.

4. Discussion

The idea of the crystallographic and electronic structure of the obtained microcontact bridges is critical for this study. The main point that largely determines the physics of the phenomena occurring in microcontacts is their size. The geometry of microcontacts can be estimated based on the magnitude of their electrical resistance based on the approach developed by Yu.V.Sharvin [22], and the approach used in measuring the hardness of materials. In the last approach, the contact size is determined by the hardness of the material and the force with which the indenter is pressed into the material. Hardness is measured by the amount of pressure that a material withstands. There is information in the literature about the hardness of europium hexaboride [20], whereas the hardness of the different facets of a single crystal, like that of a diamond crystal, has differences. According to [20] the facet [110] has a hardness of $h_{(110)}$ 41.67 GPa, while the facet [100] has a way lesser hardness $h_{(100)}$ 29 GPa. A brass rod (elasticity coefficient 95 H/m) with a section of $2\times0.1\,\text{mm}^2$ having the end shifted by 1 mm and the arm of 10 mm provides a load of $P_{(111)} \sim 0.19\cdot10^{-3}$ N applied to the indenter. This, with the above-mentioned face [100] hardness, gives an impression with an area of $0.66\cdot10^{-14}\,\text{m}^2$ in the form of an equilateral triangle with a side of 123 nm or the corresponding nominal diameter of D microcontact of about 91 nm.

The resistance of Sharvin contact, according to [22], defined as $R_{Sh} = (v_f m_e)/(ne^2\cdot D^2)$, where v_f — Fermi velocity, m_e — mass of the electron, e — charge of the electron, n — electrons concentration, D — contact diameter. The resistivity of the bulk material in the free electron gas approximation is expressed by the similar formula $\rho = (v_f m_e)/(ne^2\Lambda)$, where Λ is the electron mean free path. From these expressions the contact diameter may be estimated as $D_{\text{Sh}} = (\Lambda\cdot\rho/R_{\text{Sh}})^{1/2}$. Since the same current flows through the bulk crystal and the microcontacts, then

(not taking into account the currents flowing through the devices and the voltage drop across the silver paste holding the potential Al-wire on the bulk crystal and the silver paste holding the indenter crystal), the ratio ρ/R_{Sh} is itself the ratio of potentials on the structure's low-resistance and high-resistance parts allowing for the geometry determined by the cross-sectional area ($0.8\times2.0\,\mathrm{mm}^2$) of the bulk crystal and the distance between potential contacts on it. For the temperature of 303 K this ratio (with dimensions) we got $\rho/R_{\mathrm{Sh}} = 51\,\mathrm{m}$. There is no data on the electron mean free path in pure europium hexaboride in the studied literature. Assuming the electron mean free path may be $\Lambda \sim 10\,\mathrm{nm}$, we get a diameter of $D_{\mathrm{Sh}} \sim 71\,\mathrm{nm}$ for the Sharvin contact.

To completely match the diameter of the contact, estimated based on the hardness of faces $\{100\}$, the mean free path Λ should have been taken 16 nm.

It should also be emphasized once again that the second indenter contact sagged when excessive current was passed, which resulted in the contact resistance decline by ~ 2 times and its diameter appropriate increase by $\sqrt{2}$ times, i. e. to $100-125\,\mathrm{nm}$. Also, given rather arbitrary nature of estimates of the indenter-contact pressing force, the correlation between various estimates of the microcontact diameter and the mean free path seems to be good and consistent with reality.

In the paramagnetic state, as it was found in [23–25], anisotropy of magnetization occurs. This effect can hardly be attributed to a feature of a spin nematic [12,13,16]. However, if we believe that when this system is in the paramagnetic state, apart from the magnetization anisotropy, there are also anisotropy of the paramagnetic Curie temperature, impact of impurities enhancing antiferromagnetism, latent antiferromagnetism [12,25] (which may be considered as manifestations of a quantum nematic transition) observed, and also given that the magnetic field direction impacts the paramagnetic Curie temperature because of some deeper reasons related to exchange interactions in the electronic system of europium hexaboride, then we may say almost for sure, that a quantum nematic may occur in EuB_6.

These observations [23–25] were published in 2012, and it was almost impossible at that time to strictly relate them to the concept of a quantum nematic. At the same time, it now seems that this may be characteristic of many europium compounds, since the nematic behavior is associated with high-spin states of magnetic ions [14–16]. This also includes the polaronic states in EuB_6, which, in principle, can form two nematic phases.

It should be stressed that in [12,25] a latent antiferromagnetism of EuB_6 is observed in the exchange interactions of localized spins, and in [12] the indistinguishability of the magnetic properties of spin nematic and antiferromagnetic is emphasized, as well as the existence of two types of the spin nematic.

The literature indicates a strong influence of impurities and structural defects on the properties of EuB_6 while maintaining the cubic structure of the stoichiometric EuB_6. This circumstance primarily suggests that the microcontact material may differ from the source material. However, all manipulations with the heating of microcontacts were performed in an atmosphere of pure gaseous helium produced by evaporation of liquid helium. In addition, it is noted in [21] that under indenter pressure, a shear amorphization of the crystal structure occurs only with the rupture of individual boron-boron bonds in B_6 — octahedra. That is, with the pressure relief the crystalline structure in the shear area gets restored. Also, considering that positions of singularities on the magnetoresistance temperature dependences for both contacts are at the same values as for the bulk material (15.5 K), it may be concluded that the material of both microcontacts does not significantly differ from the bulk material. This means that more than a ~ 2 time difference in resistance of microcontacts may be explained by more than a $\sqrt{2} \sim 1.4$ time difference in their sizes.

From the most general considerations, the following should be noted. In a strict sense, magnetic susceptibility is not a scalar quantity such as mass or charge, but a tensor that characterizes the magnetic medium and connects the magnetization vector with the magnetic field strength vector. That is, in case when this tensor has only diagonal components that are not zero, we have a standard primitive representation and the susceptibility can be considered as a scalar connecting the components x, y, z of the magnetization vector with the same components x, y, z of the magnetic field strength vector. Since the non-diagonal components of the magnetic susceptibility tensor are not equal to zero, it indicates that the exchange interactions in the magnetic moments system become a way more complicated and the paramagnetic Curie temperature, as a value related to the first derivative of the magnetic energy temperature, generally becomes dependent on the direction of the external magnetic field.

No doubt that quantum nematicity is a physical state that exists under certain conditions, and the transition to this state is itself a quantum phase transition. That is, the pressure–magnetic field–composition–temperature diagrams should have corresponding quantum critical points that establish the boundaries of the existence of the magnetic phase according to certain characteristics. Such a sign could be the presence of nonzero non-diagonal components in the magnetic susceptibility tensor. Apparently, the simplest indication that we are dealing with such a magnetic susceptibility tensor is the observed anisotropy of the paramagnetic Curie-Weiss temperature T_c. In case of EuB_6, anisotropy of the paramagnetic Curie temperature T_c is indeed observed (evidence of latent AFM), which (e.g., when doped with carbon) may have a sign opposite to that of the magnetic ordering and depend on the direction of the magnetic field.

Assuming that complete degradation (suppression) of magnetoresistance occurs when the sample size is compared with the correlation length of the magnetic (nematic) phase, this length then can be estimated based on the microcontacts magnetoresistance data illustrated in Figures 2 and 3.

Linear extrapolation to zero magnetoresistance and magnetoresistance of the bulk sample yields a correlation length in the range of 50−70 nm, whereas transition to the „bulky" behavior being occurred with the size corresponding to the two correlation lengths. Considering that the polaron is estimated in [6] to be around 0.82 nm in size, this correlation length is not related to the transition to the polaron state and can be attributed to a higher temperature range, from which the values of the paramagnetic Curie-Weiss temperature for various crystallographic directions are analyzed.

5. Conclusion

The nature of the measured temperature dependences indicates the absence of any such microcontact heating effects, that a shift in the singularities of these dependences along the temperature scale could be expected. The positions of singularities on the temperature dependence — i.e. the maximum magnetic resistance and the start of the curve deviation from zero line — are the same as previously obtained in magnetic resonance measurements. However, the relative magnetoresistance, the magnitude of the effect, turn out to be significantly less in the microcontacts. This may be due to a lower number of carriers in the microcontact and their strong scattering in the transition region, where the crystallographic direction changes from [111] to [001], or due to pinning of the polarons magnetization on the contact surface, which makes it difficult for the magnetic field to reorient the polarons along the correlation length of the nematic phase, which is estimated from the obtained dependencies on the microcontacts size as 50−70 nm. That is, when the microcontact is 50−70 nm in size and when the magnetic field of 780 mT is applied, there are no any changes in its small-scale magnetic phase structure, whereas with the size of 100−130 nm, the microcontact behaves almost just like the bulk material. This finding indicates the possibility of localizing polarons in mesoscopic EuB_6 structures and treating them as independent physical objects.

Acknowledgments

The author thanks Natalia Yu. Shitsevalova (Institute of Problems of Materials Science named after I.M.Frantsevich NASU) for providing (2010) the initial materials for the preparation of europium hexaboride microcontacts; laboratory of Microcontact Spectroscopy of the Institute of Low Temperature Physics in NASU (Head of laboratory I.K. Janson) and Professor of the Department of Low Temperature Physics and Superconductivity, Lomonosov Moscow State University, Ya.G. Ponomareva for the „first-hand" consultations (2005) on microcontact spectroscopy of superconductors and magnetics.

Funding

This study was carried out under the state assignment № EGISU 125031903979-7 „Physics of functional materials and hybrid mesoscopic structures for microelectronics, energy and information technologies" Supervisor L.R. Tagirov

References

[1] I.Ya. Korenblit, E.F. Shender. UFN, **126** (233), 1978 (in Russian).
[2] E.L. Nagaev. UFN, **166**(833), 1996 (in Russian).
[3] M.Yu. Kagan, K.L. Kugel. UFN, **171** 577 (2001) (in Russian).
[4] M.Yu. Kagan, A.V. Klaptsov, I.V. Brodsky, K.I. Kugel, A.O. Sboychakov, A.L. Rakhmanov. UFN, **173**, (877) (2003) (in Russian).
[5] Stephanie A. Getty. Electron transport studies of the ferromagnetic semiconductor calcium hexaboride, a dissertation presented to the graduate school of the University of Florida in partial fulfillment of the requirements for the degree of doctor of philosophy, University of Florida, 2001, 136 pages.
[6] M.A. Anisimov, A.V. Bogach, A.V. Kuznetsov, A.N. Azarevich, N.A. Samarin, S.V. Demishev, N.Yu. Shitsevalova, A.V. Dukhnenko, V.B. Filipov, N.E. Sluchanko, V.V. Glushkov. FTT, **61**, 688(2019) (in Russian).
[7] V.A. Atsarkin, V.V. Demidov. ZhETF, **130**, 677(2006) (in Russian).
[8] Chul-Hee Min, Boyoun Kang, Beong Ki Cho, En-Jin Cho, Byeong-Gyu Park. J. of the Korean Phys. Soc.,**79**, 734 (2021), doi:10.1007/s40042-021-00273-1.
[9] M.J. Calderón, L.G.L. Wegener, P.B. Littlewood. Phys. Rev. B **70**, 092408 (2004), doi: https://doi.org/10.1103/PhysRevB.70.092408.
[10] M.L. Brooks, T. Lancaster, S.J. Blundell, W. Hayes, F.L. Pratt, Z. Fisk. Phys. Rev. B **70**, 020401(R) (2004). doi: https://doi.org/10.1103/PhysRevB.70.020401.
[11] Adham Amyan, Pintu Das, Jens Müller, Zachary Fisk. J. of the Korean Phys. Soc., **62**, 1489 (2013). doi: 10.3938/jkps.62.1489.
[12] A.F. Andreev, I.A. Grischuk. ZhETF, **87**, 467 (1984) (in Russian).
[13] G. Beaudin, L.M. Fournier, A.D. Bianchi, M. Nicklas, M. Kenzelmann, M. Laver, W. Witczak-Krempa. Phys. Rev. B **105**, 035104 (2022).
[14] E.V. Orlenko, F.E. Orlenko. FTT **58**, 1338 (2016) (in Russian).
[15] O.A. Kosmachev. Scientific reports of Tavrida National University named after V.I. Vernadsky, Series „Fiziko-matematicheskiye nauki" **25**, *64*, 59 (2012) (in Russain).
[16] Ya.Yu. Matyunina, O.A. Kosmachev, Yu.A. Fridman. Fizika metallov i metallovedenie (in Russian) **125**, 521 (2024) (in Russian).
[17] A.O. Sboychakov, K.I. Kugel, A.L. Rakhmanov. Phys. Rev. B **76**, 195113 (2007).
[18] L.M. Falicov, J.C. Kimball. Phys. Rev. Lett. **22**, 997 (1969).
[19] Tanmoy Mondal, Pinaki Majumdar., Phys. Rev. B **111**, 195103 (2025), doi: https://doi.org/10.1103/PhysRevB.111.195103
[20] A.I. Akimenko, I.K. Janson. Pisma ZhETF —bf31, 209 (1980) (in Russian).

[21] Rajamallu Karre, Yidi Shen, Shuangxi Song, Yixuan Hu, Simanta Lahkar, Xiaodong Wang, Qi An, Kolan Madhav Reddy. Communications materials, **3**, 24 (2022). https://doi.org/10.1038/s43246-022-00246-2
[22] Yu.V. Sharvin. ZhETF **48**, 984-985 (1965) (in Russian).
[23] Yu.V. Goryunov, A.V. Levchenko. J. of Phys.: Conf. Series **391**, 012014 (2012). doi:10.1088/1742-6596/391/1/012014
[24] T.S. Altshuler, Yu.V. Goryunov, N.Yu. Shitsevalova, A. Dukhnenko. J. of Phys.: Conf. Series **200**, 032019 (2010). doi:10.1088/1742-6596/200/3/032019
[25] T.S. Altshuler, Yu.V. Goryunov, N.Yu. Shitsevalova, V.B. Filippov. Appl. Magn. Reson. **46**, 25(2015). doi: 10.1007/s00723-014-0598-3

Translated by T.Zorina